PROTEINS: Structure, Function, and Genetics 50:341–354 (2003)

Differential Scanning Calorimetric, Circular Dichroism, and Fourier Transform Infrared Spectroscopic Characterization of the Thermal Unfolding of Xylanase A from *Streptomyces lividans*

Martin Roberge, [1,2] **Ruthven N.A.H. Lewis,** [3] **François Shareck,** [1] **Rolf Morosoli,** [1] **Dieter Kluepfel,** [1] **Claude Dupont,** [1] **and Ronald N. McElhaney,** [3*]

[1]*Centre de Recherche en Microbiologie Appliquée, Institut Armand-Frappier, Laval, Quebec, Canada*
[2]*Protein Engineering Department, Genentech Inc., San Francisco, California*
[3]*Department of Biochemistry, University of Alberta, Edmonton, Alberta, Canada*

ABSTRACT **The thermal unfolding of xylanase A from *Streptomyces lividans*, and of its isolated substrate binding and catalytic domains, was studied by differential scanning calorimetry and Fourier transform infrared and circular dichroism spectroscopy. Our calorimetric studies show that the thermal denaturation of the intact enzyme is a complex process consisting of two endothermic events centered near 57 and 64°C and an exothermic event centered near 75°C, all of which overlap slightly on the temperature scale. A comparison of the data obtained with the intact enzyme and isolated substrate binding and catalytic domains indicate that the lower- and higher-temperature endothermic events are attributable to the thermal unfolding of the xylan binding and catalytic domains, respectively, whereas the higher-temperature exothermic event arises from the aggregation and precipitation of the denatured catalytic domain. Moreover, the thermal unfolding of the two domains of the native enzyme are thermodynamically independent and differentially sensitive to pH. The unfolding of the substrate binding domain is a reversible two-state process and, under appropriate conditions, the refolding of this domain to its native conformation can occur. In contrast, the unfolding of the catalytic domain is a more complex process in which two subdomains unfold independently over a similar temperature range. Also, the unfolding of the catalytic domain leads to aggregation and precipitation, which effectively precludes the refolding of the protein to its native conformation. These observations are compatible with the results of our spectroscopic studies, which show that the catalytic and substrate binding domains of the enzyme are structurally dissimilar and that their native conformations are unaffected by their association in the intact enzyme. Thus, the calorimetric and spectroscopic data demonstrate that the *S. lividans* xylanase A consists of structurally dissimilar catalytic and substrate binding domains that, although covalently linked, undergo essentially independent thermal denaturation. These observations provide valuable new insights into the structure and thermal stability of this enzyme and should assist our efforts at engineering xylanases that are more thermally robust and otherwise better suited for industrial applications. Proteins 2003;50:341–354.**

Key words: xylanase A; *Streptomyces lividans*; thermal unfolding; protein denaturation; domain interactions; differential scanning calorimetry; circular dichroism; infrared spectroscopy

INTRODUCTION

The β-1,4-endoxylanase xylanase A (XlnA) from the mesophylic actinomycete *Streptomyces lividans* is a member of a class of polysaccharidases being investigated by the pulp and paper industries for their potential use in the biobleaching of wood pulp and for other applications in the textile, biomass energy, and chemical industries.[1–3] The use of these enzymes in various industrial processes often requires the retention of enzyme activity in liquid environments at relatively high temperatures and on occasion at extremes of pH or ionic strength. The successful application of naturally occurring or engineered xylanases in such processes thus requires a detailed knowledge of enzyme structure and activity over a range of temperatures, pHs, and salt concentrations, all as a function of time, in both the presence and absence of substrate. Investigations of the thermal stability of xylanases and related enzymes under various conditions are thus important in this regard because such studies can provide fundamental insights

Abbreviations: CD, circular dichroism; DSC, differential scanning calorimetry; FTIR, Fourier transform infrared; XlnA, xylanase A; XCD, catalytic domain of xylanase A; XBD, xylan binding domain of xylanase A; T_m, temperature at which 50% of the protein is unfolded; ΔH, enthalpy change; ΔS, entropy change; ΔCp, heat capacity change.

*Correspondence to: Ronald McElhaney, Department of Biochemistry, University of Alberta, Edmonton, Alberta T6G 2H7, Canada. E-mail: rmcelhan@gpu.srv.ualberta.ca

Received 26 January 2002; Accepted 4 June 2002

into the forces stabilizing the structure and function of the native enzyme, information that can potentially also be of considerable commercial value.

The XlnA from *S. lividans* is a secreted enzyme that is responsible for the hydrolysis of xylan into small oligoxylosides that can be further broken down by this fungal species and the products utilized as carbon and energy sources.[4] The native *S. lividans* Xln A exhibits its optimal activity at a temperature of 60°C at pH 6.0, which makes it potentially suitable for the biobleaching of wood pulp; however, the half-life of XlnA under these conditions is only about 130 and 320 min in the absence and presence of substrate, respectively.[5] Moreover, for some applications it would be desirable to have an engineered XlnA that could function at higher temperatures and at different pH values. Thus, we cloned[6] and sequenced[7] the gene for XlnA and developed an efficient overexpression system for this gene in both *S. lividans* and *Escherichia coli.*[6] Using site-specific mutagenesis, we also identified a number of amino acid residues that are required for the enzyme activity and thermal stability of XlnA and are proceeding to engineer mutant enzymes with more desirable properties.[5,8–10] We believe that the results of the present study of the thermostability of the native enzyme will provide information that we can utilize in this endeavor.

XlnA from *S. lividans* is a 47-kDa protein with a pI of 5.2.[4] It is a modular protein consisting of two discrete structural and functional units, a 33-kDa N-terminal catalytic domain (XCD) and a C-terminal substrate binding domain (XBD). The XCD is a member of family 10 of the glycosyl hydrolases[7] and the XBD is a member of family XI of the cellulose binding domains[11] according to their amino acid sequences. Although a high-resolution structure for the intact enzyme is not yet available, we determined the structure of the isolated XCD domain, which folds into an $(\alpha\beta)_8$ barrel motif.[12] Moreover, based on the structures of the catalytic and substrate binding domains of the closely related β-1,4-glycanase from *Cellulomonas fimi,*[13,14] it is likely that the XCD and XBD domains of XlnA from *S. lividans* are connected by a linker peptide that may inhibit direct interactions between the two domains in the intact protein. Thus, one of the goals of the present study is to investigate the extent to which the interaction of these domains alters the thermal stability in the intact enzyme.

In this study we employ differential scanning calorimetry (DSC) to investigate the thermal stability of intact XlnA and its isolated XCD and XBD domains in aqueous solutions at various pHs and ionic strengths. Although this technique is a powerful one that can provide reliable information about the thermodynamics and reversibility of protein unfolding, it does not provide direct structural information.[15] Therefore, we supplemented our DSC analyses with both circular dichroism (CD) and Fourier transform infrared (FTIR) spectroscopic studies to gain some insight into the overall conformational changes that accompany the thermally induced unfolding of this enzyme and of its isolated domains.

MATERIALS AND METHODS

Protein Preparation and Purification

The enzyme XlnA and its XCD were prepared as described by Bertrand et al.[6] and Derewenda et al.,[12] respectively, and were purified as described previously.[5] The material prepared was assayed for enzymatic activity[5] and the specific activity values obtained were consistent with those expected of pure, fully functional enzyme (data not shown). The XBD domain was prepared and purified as described by Dupont et al.[11] The protein content of the DSC and CD samples was determined from absorbance values measured at 280 nm. The measured absorbances were calibrated in terms of absolute protein content by amino acid analysis. Under our conditions (50 mM phosphate, pH 6.0), such analyses returned uncorrected $\epsilon 280$ extinction coefficients of 104,280, 68,420, and 33,870 for the native protein and its XCD and its XBD domains, respectively. Our experimentally determined values compare favorably with theoretical estimates of 97,500, 64,490, and 33,010, respectively, as calculated by the procedures developed by Gill and von Hippell.[16]

DSC

Samples were prepared for DSC experiments by dissolving 1–2 mg of the pure lyophilized protein in 1.8 mL of appropriate buffer. Such concentrations are high enough to give unfolding endotherms of acceptable signal-to-noise ratios while minimizing distortions of the endotherms by thermotropic events related to the aggregation of unfolded protein. The pH dependence experiments were performed in 50 mM buffers. These were prepared by titrating appropriate amounts of 50 mM citric acid with 50 mM Na_2HPO_4 (pH $<$ 6.0), 50 mM NaH_2PO_4 with Na_2HPO_4 (pH 6.0–8.0), and 50 mM sodium borate with 50 mM NaH_2PO_4 (pH $>$ 8.0). All buffers also contained 1 mM NaN_3, a bacterial growth inhibitor. The variations in the ionic strengths of these buffers are not a significant factor in these experiments because our preliminary experiments indicate that the thermal unfolding of these proteins is essentially insensitive to variations in ionic strength over the range 5–500 mM salt. Most of the DSC thermograms were recorded with a computer-controlled MC-2 high-sensitivity calorimeter (Microcal Inc., Amherst, MA) operating at scan rates of 18°C/h and with a digital encoding frequency of 8 s. A few measurements were also performed on a Microcal VP-DSC instrument operating at scan rates near 30°C/h. For the DSC experiments, at least two heating thermograms were recorded with each sample at temperatures between 5 and 90°C. The first thermogram, which contains endotherms arising from protein unfolding and exotherms arising from aggregation, was used to obtain thermodynamic data related to those events. A subsequent thermogram containing none of the aforementioned thermotropic events was used as a reference baseline. With the XCD and the intact XlnA thermograms, two heating scans were usually acquired, whereas with the XBD at least three heating thermograms between 5 and 90°C were required before thermograms free of all protein-related thermotropic events were obtained. With experiments designed to evaluate the thermal reversibility of the

unfolding process, at least three heating thermograms were recorded. The first was recorded between 5°C and a predetermined temperature commensurate with the degree of thermal unfolding required. The sample was then immediately recooled to 5°C and, after an appropriate time for thermal equilibration, two or more DSC thermograms were recorded between 5 and 90°C. The last of these thermograms was used to construct a sample baseline. Typically, data processing involved the interpolation of a smooth, adjacent averaged baseline from the second (or final) thermogram recorded and the subtraction of this baseline from the first thermogram. The data obtained could then be used for plotting and/or deconvolution using standard scientific data analysis and plotting packages. In our case, data analysis was performed using the Origin software package (OriginLab Corp., Northampton, MA) and the deconvolution of the unfolding endotherms into component thermograms was achieved with the Origin peak-fitting module. The peak-fitting routines used a custom-coded function that treats DSC thermograms as idealized, first-order, two-state process at thermal equilibrium. Curve fitting was based on the assumption that the observed DSC thermogram is a summation of multiple independent thermotropic events, each of which can be approximated by a two-state process.

FTIR Spectroscopy

Samples for FTIR spectroscopy were prepared by dissolving 1–2 mg of the lyophilized protein sample in 50 μL of a D_2O-based buffer (50 mM phosphate, 1 mM NaN_3, pH 6.0). The solution was then sealed as a thin (25 μm) film between the CaF_2 windows of a heatable, demountable liquid cell equipped with a 25-μm Teflon spacer. Once mounted in the sample holder of the instrument, sample temperature could be controlled between −20 and 90°C by means of an external, computer-controlled water bath. FTIR spectra were recorded with a Digilab FTS-40 Fourier-transform spectrometer (Biorad, Digilab Division, Cambridge MA) using the data acquisition parameters described by Mantsch et al.[17] The data were analyzed by computer programs obtained from Digilab Inc. and from the National Research Council of Canada. In cases where spectra appear to be a complex summation of component bands, Fourier self-deconvolution procedures were used to obtain estimates of the frequencies of the component bands. Typically, this was achieved using band narrowing factors of 1.5–2.2 and band widths ranging from 20–30 cm^{-1}. Under our conditions, band narrowing factors of up to 2.5 could be used without introducing significant distortions into the deconvolved spectra. Subsequently, curve-fitting procedures were employed to estimate the widths and intensities of the components identified above by reconstructing the contours of the original absorption band. This was achieved by a linear combination of the components identified by Fourier deconvolution with the aid of standard nonlinear, least-squares minimization procedures. Each component was simulated by a Gaussian–Lorentzian function for which best-fit estimates were typically achieved with Gaussian contribution near 70%.

CD

Far-UV CD spectra were recorded on a computer-controlled Jasco J-720 CD spectropolarimeter using a path length of 0.019 cm, a digital resolution of 0.2 nm, a scan speed of 50 nm/min, and a response time of 0.25 s. Spectra were recorded with samples (≈ 0.5 mg/mL protein) dissolved in 50 mM phosphate buffer (pH 6.0). The spectral data presented are in units of mean residue molar ellipticity values, obtained by the signal averaging of 10 spectra, and have been corrected by subtracting the buffer spectrum. The instrument was calibrated with an aqueous solution of recrystallized $d_{10}(+)$-camphor sulfonic acid at 290.5 nm. For the thermal denaturation experiments, samples (≈ 0.5 mg/mL) were heated in a 0.05-cm jacketed cell at a rate of 0.5°C/min from 45–85°C using a Neslab 110 programmable water bath. Changes in XlnA and XCD structure due to unfolding were followed at 210 nm at every 0.2°C, while unfolding of the XBD was followed at 230 nm under the same conditions. The data obtained for thermal denaturation curves were transformed into fraction of unfolded protein according to the following equation, assuming a two-state unfolding mechanism

$$fD = X - X_N / X_D - X_N$$

where X_N is the value of folded protein, X_D the value for the unfolded protein, and X the value observed. The thermodynamic parameters were calculated using procedures described by Pace et al.[18] For the determination of the effect of pH on the thermal denaturation of XlnA, the enzyme was dissolved in citric acid–sodium phosphate buffer 50 mM (pH 4.0–5.5), in sodium phosphate buffer 50 mM (pH 6.0–8.0), and in boric acid–NaOH buffer 50 mM (pH 8.5–9.0).

RESULTS

DSC (General Features)

Representative high-sensitivity DSC heating thermograms of samples of *S. lividans* intact XlnA and isolated XBD and XCD dissolved in aqueous buffer at pH 6.0 are shown in Figure 1. It is clear that under these conditions the native XlnA exhibits DSC thermograms that contain two overlapping endothermic components. These endotherms are centered near 57 and 64°C, respectively, and the lower-temperature component is the broader and less energetic of the two events. In contrast, the DSC thermograms exhibited by the isolated XBD and XCD each contain a single endotherm, centered near 57 and 64°C, respectively, and their widths and midpoint temperatures are comparable to those of the lower- and higher-temperature endothermic components observed in the DSC thermograms of the intact enzyme. Thus, the endothermic events centered near 57 and 64°C in the native enzyme must arise from the independent thermal unfolding of the XBD and XCD domains, respectively.

A close inspection of Figures 1(A) and 1(C) indicates that the DSC endotherms corresponding to the thermal unfolding of the catalytic domain, either in the intact enzyme or in isolated subunit, also exhibit an exothermic event that begins at temperatures near the completion temperature of the endothermic unfolding event. Comparable exother-

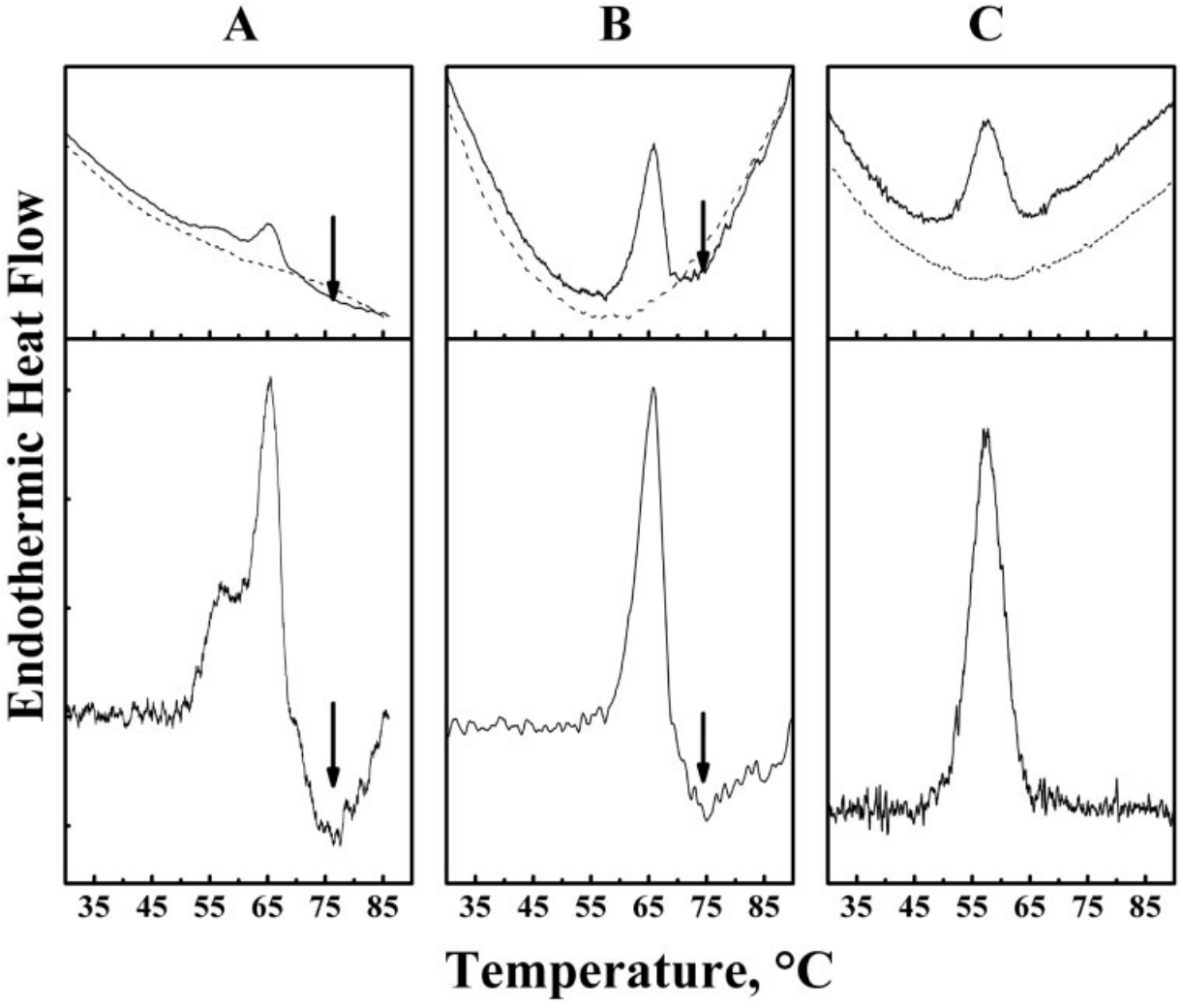

Fig. 1. Representative DSC thermograms observed during the thermal unfolding of *S. lividans* xylanase A. The data shown were obtained from samples dissolved in 50 mM phosphate buffer at a pH of 6.0 and are representative of the intact enzyme (**A**), the catalytic domain (**B**), and the xylan binding domain (**C**). The top panels show thermograms observed during the unfolding of the protein (solid lines) and those obtained in subsequent heating scans after complete suppression of all protein-related thermotopic events (broken lines). The data shown in the bottom panels are the unfolding thermograms after baseline subtraction. The arrows indicate the positions of exothermic events attributed to aggregation phenomena.

mic events were not observed in the unfolding thermograms exhibited by the XBD. Such exothermic events are usually correlated with the aggregation and precipitation of largely denatured proteins, consistent with our observation that both the XlnA and the isolated XCD precipitate irreversibly when heated to temperatures above 70–75°C. The appearance of an exothermic event in close proximity to the unfolding transitions of the native protein and of its catalytic domain thus raises the possibility that the observed unfolding endotherms may have been distorted by a significant overlap of the unfolding and aggregation processes. To address this issue, DSC studies were performed with XCD and XBD to evaluate the potential reversibility of the thermal unfolding process. In addition, FTIR spectroscopy was used to evaluate the extent of overlap of the temperature ranges over which the unfolding and aggregation processes occur. The latter technique and CD spectroscopy were also used to obtain additional information about the secondary structure of XlnA, its isolated substrate binding and catalytic subunits, and the changes in secondary structure that accompany their thermal unfolding.

Illustrated in Figure 2 are DSC thermograms of the thermal unfolding of the XBD of *S. lividans* XlnA. The data obtained are summarized in Table I. It is clear that the xylan binding domain unfolds completely when heated to temperatures near 68.7°C [Fig. 2(A)]. Also, if immediately recooled from such temperatures, the succeeding DSC thermogram exhibits an unfolding endotherm that is essentially indistinguishable from that observed initially [see Fig. 2(A,B)]. This result provides strong evidence that the thermal unfolding of the XBD is thermally reversible. It also suggests that the refolding of unfolded XBD to its native state is kinetically and/or themodynamically favored over other refolding motifs. However, when samples of unfolded XBD are heated to temperatures near 90°C succeeding DSC thermograms progressively exhibit unfolding endotherms whose enthalpy is reduced by about 75% relative to that of the previous scan [see Fig. 2(B,C)].

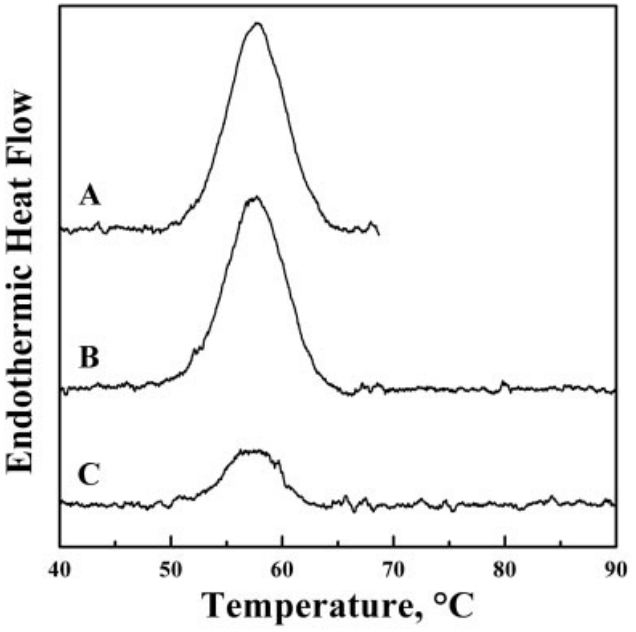

Fig. 2. DSC studies of the reversibility of the thermal unfolding of the xylan binding domain of *S. lividans* xylanase A in 50 mM phosphate buffer at pH 6.0. The data shown are DSC thermograms acquired at ≈17°C/h in three successive heating scans of the same sample. (**A**) First heating scan (5–68.5°C). (**B**) Second heating scan (5–90°C). This sample was quickly recooled to 5°C immediately after completion of scan A. (**C**) Third heating scan (5–90°C). This sample was quickly cooled to 5°C immediately after completion of scan (B).

However, the midpoint temperatures and widths of those endotherms are comparable to those exhibited by the initial unfolding endotherm. These observations suggest that the thermal unfolding and irreversible denaturation of XBD events are distinct processes and that denaturation occurs at significant rates only at temperatures above 70°C. However, significant amounts of unfolded but not irreversibly denatured XBD remain even after samples are heated to temperatures near 90°C, suggesting that the actual denaturation process may still be relatively slow even at those elevated temperatures.

DSC thermograms illustrating the results of comparable experiments with the isolated XCD are shown in panels I–III of Figure 3 and the data are summarized in Table I. These data contrast sharply those obtained from the XBD because they show that complete refolding of XCD to its native state is not observed upon either complete or partial unfolding. Also, when samples are initially heated to temperatures commensurate with high (> 60%) degrees of thermal unfolding, the areas of the unfolding endotherms observed in the succeeding DSC thermogram are significantly less than can be attributed to unfolded protein in the preceding DSC heating scan [see Table I(B)]. Clearly, the process leading to irreversible denaturation of the catalytic domain occurs more rapidly than with the substrate binding domain and commences at temperatures near to the completion temperature of the unfolding process. However, when samples of XCD are heated to temperatures commensurate with a relatively low (i.e., < 40 %) extent of thermal unfolding, the area of the succeeding DSC thermogram exceeds that expected if all of the unfolded protein remains unfolded at the termination temperature of the first DSC heating scan (see Table I). This observation suggests that reversible refolding of XCD to its native state can occur under suitable conditions.

TABLE I. Thermal Reversibility of the Unfolding of Isolated Substrate Binding and Catalytic Subunits of *S. Lividans* Xylanase A†

T_s (°C)	Estimated % Unfolding at T_s	% Total area observed in succeeding DSC scan
(A) Xylan binding subunit		
68.7	100	>95
90	100	≅25
(B) Catalytic subunit		
65.6	40	70
66.7	55	35
68.7	77	<3.0
90	100	0

†T_s, completion temperature of first DSC heating scan.

We also investigated the reversibility of the thermal unfolding of the XCD using a newer and considerably more sensitive instrument (a Microcal VP-DSC), which enabled us to obtain data of comparable quality using significantly smaller sample sizes (0.5 vs. 2.5 mL) and considerably more dilute protein concentrations (≈0.15 mg/mL vs ≈1.0 mg/mL). This study was also performed at a faster scan rate (30°C/h). The use of dilute protein solutions and the application of faster heating rates were intended to reduce the rates of aggregation of the unfolded protein by reducing the frequency of the intermolecular contacts that may trigger protein aggregation and reducing the length of time that the sample resides at high temperatures, respectively. The data presented in panel IV of Figure 3 showed that under these conditions, some 20% of the XCD protein refolded to its native state upon cooling. This result shows clearly that the unfolding and aggregation/denaturation of *S. lividans* XCD are distinct processes and that if steps are taken to reduce the rate of aggregation of the thermally unfolded protein, refolding to the native state will occur upon cooling. This result also shows that the thermal unfolding of this protein is an intrinsically reversible process. The latter conclusion is particularly important because it permits the application of standard equilibrium thermodynamic procedures for the analyses of the unfolding endotherms (see below).

FTIR Spectroscopy

Illustrated in Figure 4 are the amide I regions of the FTIR spectra exhibited by *S. lividans* XlnA, XCD, and XBD (spectra A, B, and C, respectively). The protein and its two isolated domains all show a complex pattern of amide I infrared absorption that appears to be a summation of several components. The major component of all of these spectra are absorption bands centered near 1635–1640 cm^{-1} and 1650–1655 cm^{-1}. However, these spectra also contain smaller contributions from several other

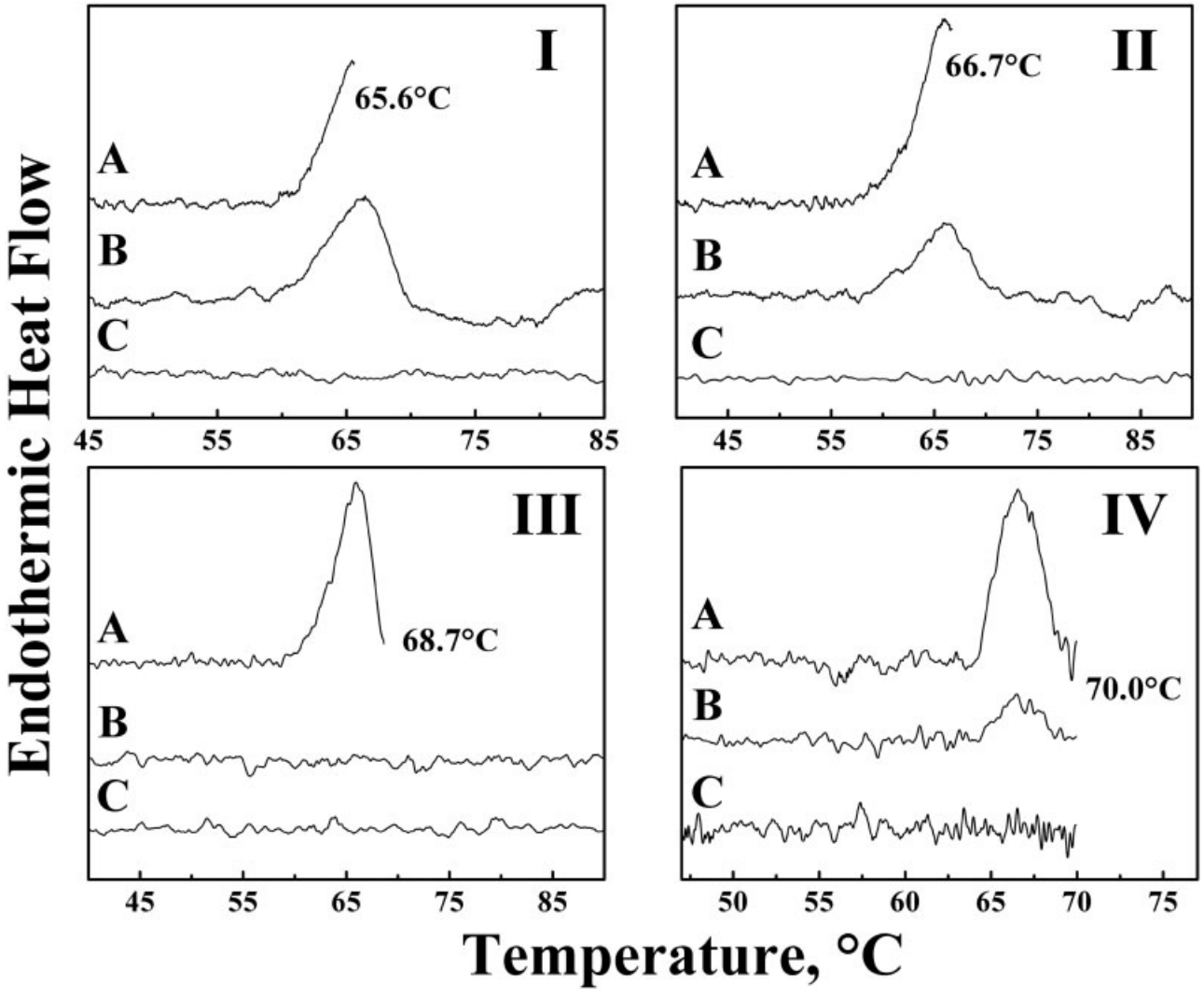

Fig. 3. DSC studies of the reversibility of thermal unfolding of the catalytic domain of *S. lividans* xylanase A in 50 mM. phosphate buffer at pH 6.0. (**I**)–(**III**) data acquired with themicrocal MC-2 calorimeter operating at scan rates of 17°C/h using 1.2-mL samples of protein concentrations near 1.0 mg/mL. (**IV**) data acquired with a more sensitive instrument (a Microcal VP-DSC) operating at scan rates near 30°C/h using samples of protein concentrations near 0.15 mg/mL. The traces of each panel represent DSC thermograms acquired in three successive heating scans of the same sample. (**I**)–(**III**): (**A**) First heating scan (5°C to temperature indicated). (**B**) Second heating scan (5–90°C). The sample was quickly recooled to 5°C after scan (A). (**C**) Third heating scan (5–90°C). The sample was quickly recooled to 5°C after scan (B). (**IV**): (**A**) First heating scan (5–70°C). (**B**) Second heating scan (5–70°C). The sample was quickly recooled to 5°C after scan (A). (**C**) Third heating scan (5–70°C). The sample was quickly recooled to 5°C after scan (B).

absorption bands, of which the most prominent are centered near 1630, 1647, and 1675 cm^{-1}. The major resolvable subcomponents identified in the amide I absorption bands of XlnA, and of its isolated catalytic and substrate binding subunits, are shown by the broken lines shown in Figure 4. The subbands shown illustrate the approximate positions and contributions of the major resolvable components and are not presented as unique curve-fitting solutions. The frequencies of the major resolvable components of XlnA and XCD are in the ranges expected of protonated α-helices (1650–1658 cm^{-1}), deuterium exchanged α-helices (≈ 1647 cm^{-1}), and nonaggregated β-sheet structures (1620–1640 and 1670–1680 cm^{-1}), respectively.[19] The signal centered at 1639 cm^{-1} could also be due to distorted helical structures (1637–1640 cm^{-1}), 3_{10}-helices (1639–1640 and 1662–1663 cm^{-1}), or parallel β-sheet structures (1637–1641 cm^{-1}),[19,20] or a combination of all these types of structures.[19,20] The latter suggestion is most compatible with the results of single-crystal X-ray diffraction studies of the catalytic domain of *S. lividans* XlnA,[12] which demonstrate the existence of all three of these conformations. Figure 4 also shows that the contours of the amide I absorption bands of the catalytic and xylan binding domains of XlnA (spectra B and C, respectively) differ significantly, indicating that there are major differences between their overall conformations. With the XBD, a large fraction of the absorbance intensity originates from components centered near 1635 and 1675 cm^{-1}, suggesting that nonaggregated β-sheet (probably antiparallel) structures are the most significant conformational motifs

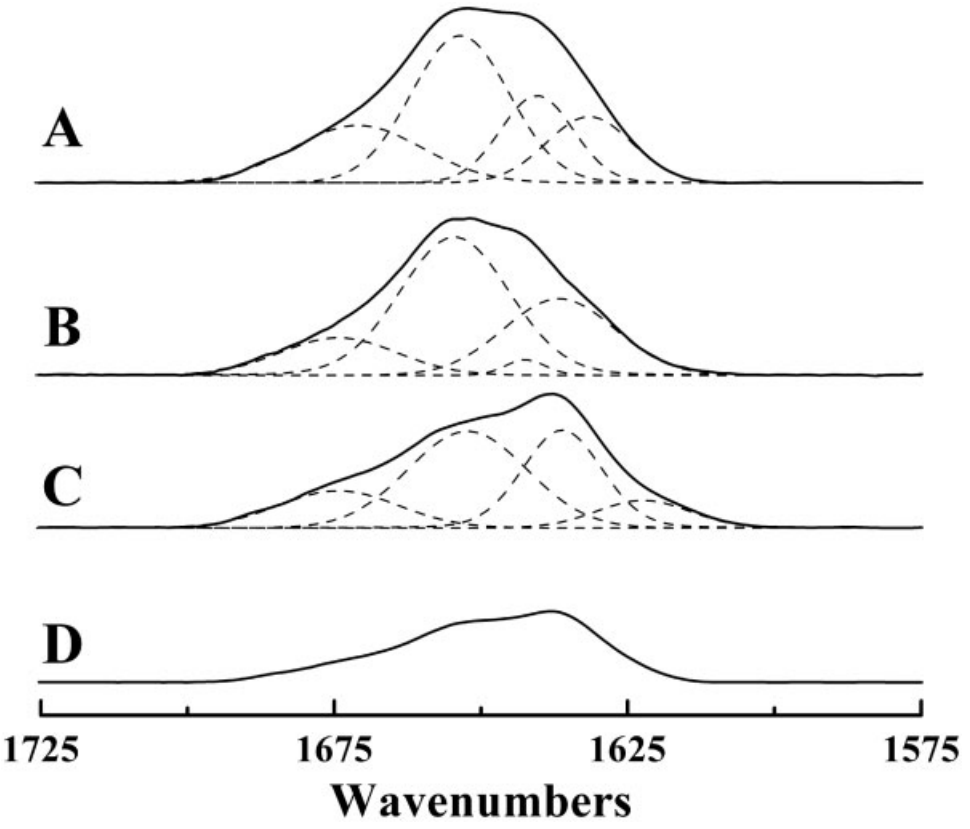

Fig. 4. FTIR absorbance spectra showing the amide I bands of *S. lividans* XlnA (**A**), XCD (**B**), and XBD (**C**). Spectrum (**D**) was obtained by a weighted subtraction of spectrum (B) from spectrum (A). The weighting of spectrum (B) was sufficient to achieve subtraction of absorbance intensity from an equivalent molar amount of XCD. The spectra shown were obtained from data acquired at 25°C and have all been solvent and baseline corrected. The solid lines represent the observed absorbance spectra and, where present, the broken lines are estimates of the major resolvable components of those spectra.

of this domain of the protein. However, the amide I band of *S. lividans* XBD may also contain a significant contribution from absorption bands centered near 1650–1655 cm^{-1}. In this case, however, it seems unlikely that the absorption arises from helical structures because the CD spectra of the protein show no evidence of significant helical content. We therefore suggest that this particular absorption band arises from unordered structural regions of the substrate binding domain, a suggestion compatible with the observation that absorption bands near 1650–1655 cm^{-1} tend to be considerably broader than those normally associated with the presence of helical structures. Finally, we note that spectra whose contours approach those of the amide I absorption band of the XBD [see Fig. 4(D)] are easily obtained by a weighted subtraction of the XCD spectra [Fig. 4(B)] from those of the native protein [Fig. 4(A)]. This suggests that the conformational motifs of the XCD and XBD in the native XlnA are essentially the same as those exhibited by each of the isolated components. This observation lends further support to the idea that the conformational stability of the catalytic and xylan binding domains of XlnA are determined by their intrinsic structures, which are not significantly affected by their association in the native protein.

Figure 5 shows various series of absorbance spectra illustrating temperature-dependent changes in the contours of the amide I bands of XlnA [5(A)] and of its catalytic [5(B)] and xylan binding domains [5(C)]. The data illustrate the spectroscopic changes observed with these protein preparations at temperatures that bracket the thermal events observed by DSC. With the native protein, the spectroscopic changes coincident with the lower-temperature thermal unfolding event consist of a growth of components centered near 1633 cm^{-1}, presumably at the expense of the components that range from 1640–1655 cm^{-1}. These observations suggest that the lower-temperature component of the DSC thermogram of XlnA (i.e., the unfolding of the XBD) probably involves a net conversion to nonaggregated β-sheet structures. This conclusion is compatible with the spectroscopic changes seen in studies of the thermal unfolding of the XBD alone [see Fig. 5(C)]. Figure 5 also shows that when the native protein or its XCD are heated to temperatures above 70°C, all of the sharp components centered between 1630 and 1655 cm^{-1} disappear and are replaced by considerably broader components centered near 1650 cm^{-1} and by two sharper components centered near 1685 and 1618 cm^{-1}. The broad components (1650 cm^{-1}) can be attributed to the formation of unordered or randomized structures and the sharp components at 1685 and 1618 cm^{-1} are consistent with the formation of aggregated β-sheet structures.[19] However, these sharp components near 1685 and 1618 cm^{-1} are not

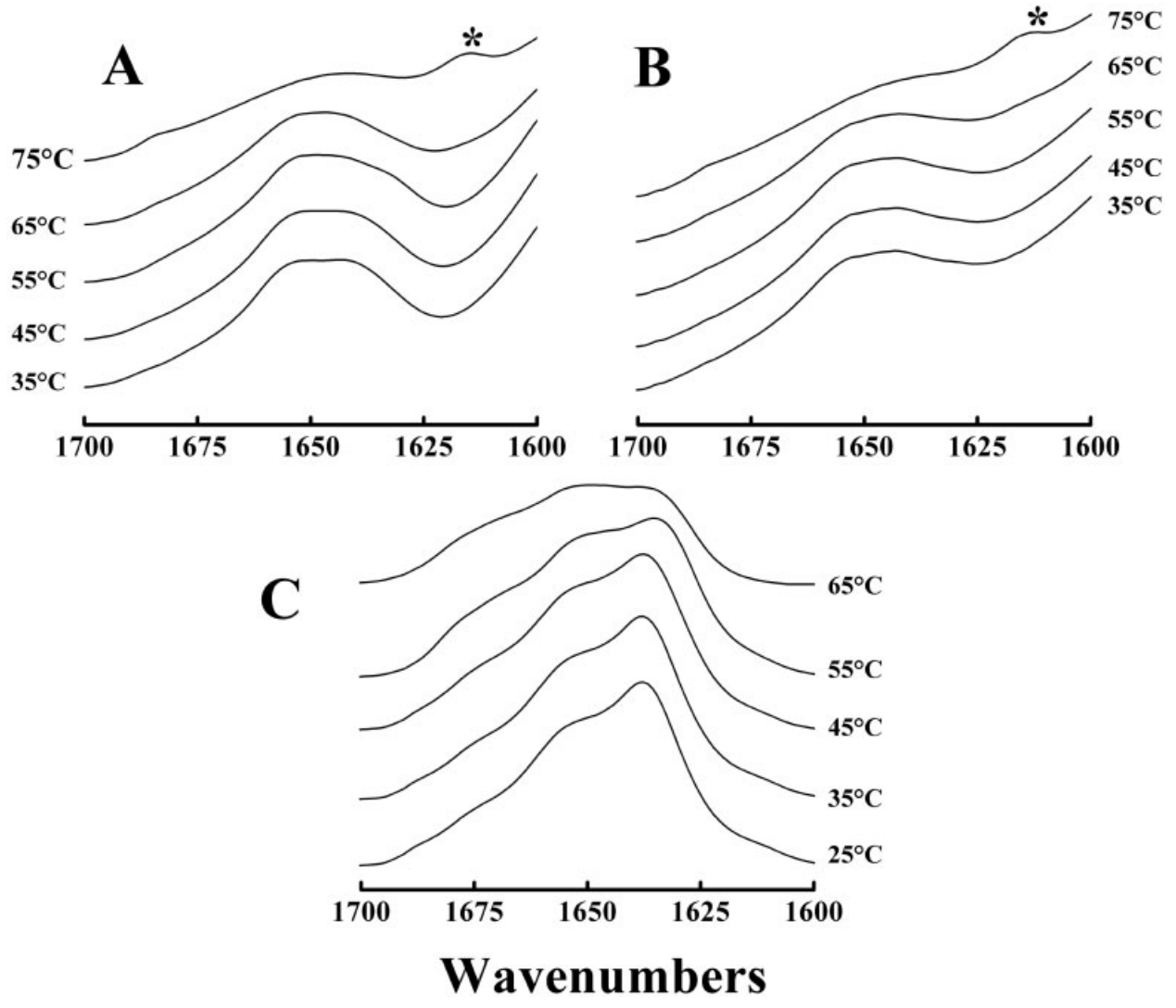

Fig. 5. FTIR spectra characteristic of the thermal unfolding of *Streptomyces lividans* XlnA (**A**), XCD (**B**), and XBD (**C**). The data shown were acquired at the temperatures indicated and represent absorbance spectra of the amide I bands of samples dissolved in the D_2O-based phosphate buffer used. Asterisks mark the position of the 1618 cm^{-1} component that appears in the high-temperature spectra of the XlnA and XlnA2 preparations. These bands have been assigned to the formation of aggregated β-sheet components (see text).

observed when the XBD is heated to temperatures well above the range of its thermal unfolding transition [see Fig. 5(C)]. These data thus provide strong evidence that aggregation phenomena are an integral part of the thermal unfolding of both XlnA and XCD, but not of the XBD, under comparable conditions. Our results also suggest that the unfolding and aggregation events that give rise to the exothermic events observed by DSC for the catalytic domain are not concurrent, although there may well be some overlap between the two processes on the temperature scale.

CD

The contours of the far-UV CD spectra of XlnA, and of isolated XCD and XCD, are shown in the left panel of Figure 6. The CD spectra of XlnA and XCD both exhibit minima near 210 and 222 nm, features that are indicative of significant helical content. However, the magnitude of their molar ellipticity values at these minima (≈9500 and 11,900 $deg.cm^2.dmol^{-1}$ for the native protein and catalytic domain, respectively) also indicates that both proteins contain significant amounts of other secondary structures. Our analyses of the CD spectra of these two proteins suggest that unordered and antiparallel β-sheet structures are also significant contributors to their overall conformation. This suggestion is compatible with the FTIR spectroscopic data presented above and with the results of single-crystal X-ray diffraction studies,[12] which show that the catalytic domain folds into a so-called $(\alpha/\beta)_8$ motif. The left panel of Figure 6 also shows that the contours of the CD spectrum of the XBD differ significantly from those of the XlnA and the XCD. Specifically, theXBD spectrum lacks the "double minima signature" normally associated with significant helical content and also contains a component that gives rise to a peak of positive molar ellipticity centered near 230 nm. The latter feature has also been

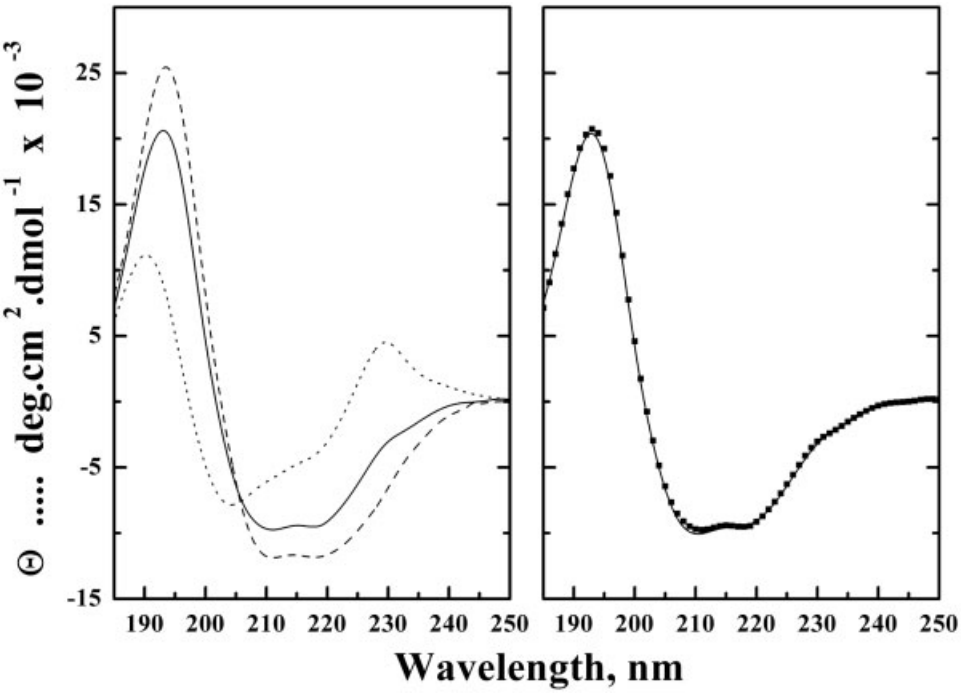

Fig. 6. Far-UV CD spectra of *S. lividans* XlnA and its isolated domains. The left panel shows the spectra exhibited by the native protein (———), the catalytic domain (- - - - -), and xylan binding domain (. . .. .). The right panel shows the CD spectrum of the native protein (filled symbols) superimposed over the spectrum obtained by a summation of those exhibited by the catalytic and xylan binding domains. All of the data shown were acquired with samples dissolved in 50 mM phosphate buffer, pH 6.0.

observed in the CD spectrum of the *Thermotoga maritima* xylanase CBD.[21] This particular feature is in general associated with the disulphide-linked and aromatic amino acid residues of proteins and is usually observed as a major feature in the CD spectra of proteins only when their secondary structures do not contain significant amounts of helix.[22,23] The CD spectrum of *S. lividans* xylanase XBD thus indicates that this subunit does not contain significant amounts of helical structure and that β-sheet and randomly ordered structures should be the predominant secondary structures present, a conclusion supported by the results of our FTIR spectroscopic studies (see above). Similar conclusions have been drawn from the results of X-ray diffraction and high-resolution NMR spectroscopic studies of the cellulose binding domains of other closely related cellulases.[24–27] Finally, we note that the contours of the CD spectrum of the XlnA can be reconstructed by an appropriately weighted summation of the CD spectra of XCD and XBD (see Fig. 6). This observation is consistent with the results of our FTIR spectroscopic studies and lends further support to the idea that the conformational motifs adopted by the catalytic and xylan binding domains in the native protein are essentially the same as those that occur in the isolated components.

Illustrated in Figure 7 are temperature-dependent changes in the ellipticities of XlnA and its isolated domains at either 210 or 230 nm, data that typify those obtained in our CD characterization of the thermal unfolding of these proteins at pH values near 6.0. With the native protein, plots of the temperature dependence of the ellipticity observed at 210 nm [for an example, see Fig. 7(A)] show a single discontinuous increase in ellipticity that coincides with the unfolding transition of the catalytic domain as observed by both DSC and FTIR spectroscopy (see above). We therefore conclude that the unfolding transition of the XBD does not result in significant changes in the ellipticity values observed near 210 nm. This conclusion is supported by the results of similar studies performed with the isolated XBD (not shown here). Interestingly, however, Figure 7 also shows that the two-component nature of the unfolding of XlnA can be detected by CD when the changes in molar ellipticity are examined at 230 nm [see Fig. 7(C)]. In this case, however, a plot of molar ellipticity as a function of temperature initially shows a discontinuous decrease in ellipticity values at temperatures centered near 57°C, followed by a discontinuous increase in those values at temperatures centered near 68°C. This observation suggests that the unfolding of the XBD is accompanied by a decrease in molar ellipticity at 230 nm, whereas the unfolding of the catalytic domain results in a net increase in molar ellipticity at the same wavelength. Currently, it is not clear why the thermal unfolding of *S. lividans* XBD is not reflected in changes in overall molar ellipticity at 210 nm, nor is it clear why the process is detectable at 230 nm, a wavelength distant from those in general presumed to carry significant structural information. Nevertheless, this conclusion is supported by the results of similar studies performed with the isolated XCD and with the isolated XBD [Figs. 7(D) and (B), respectively] and is also consistent with the idea that the thermal

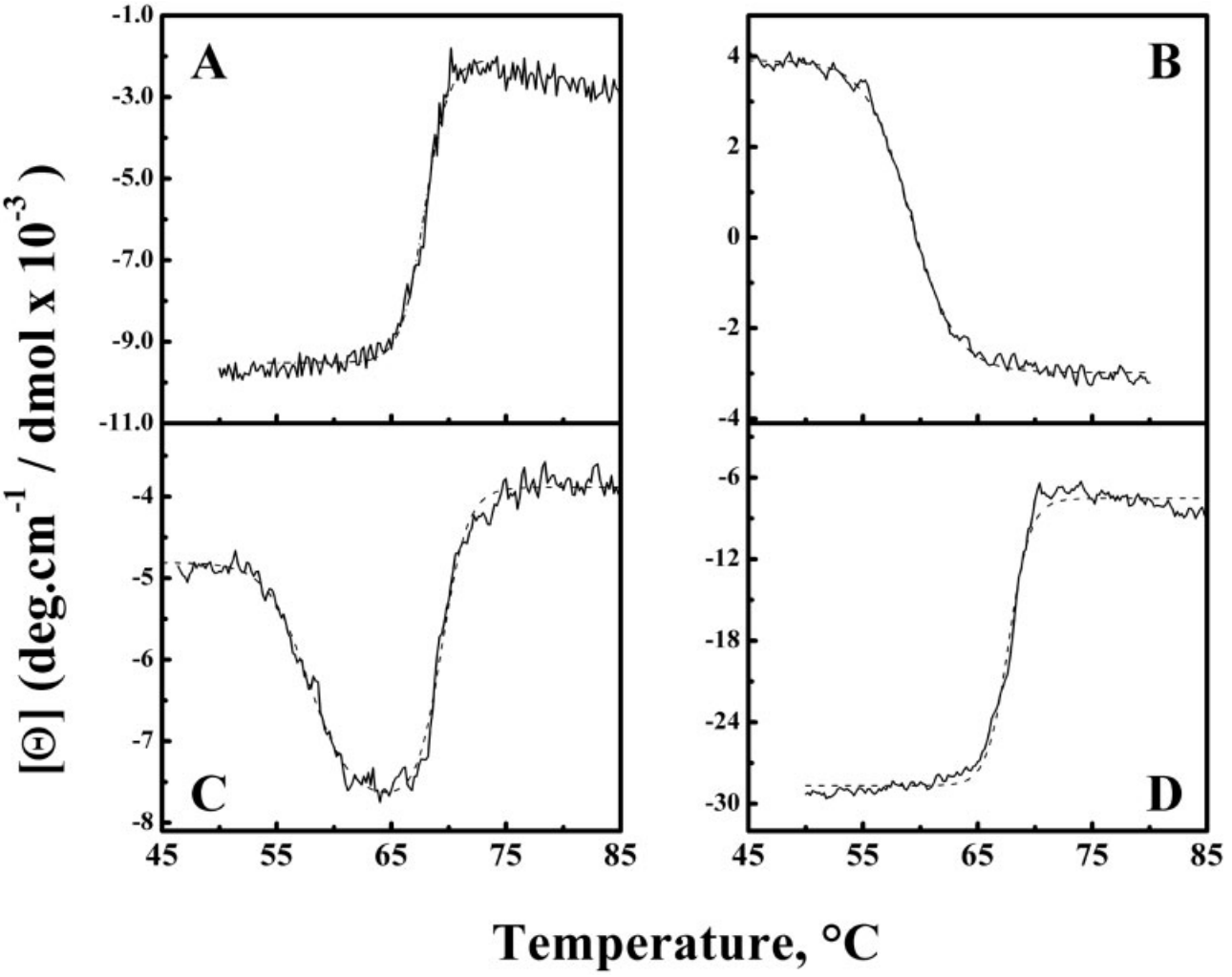

Fig. 7. Representative thermal unfolding profiles of *Streptomyces lividans* XlnA and its isolated domains as observed by CD spectroscopy. The data shown are: (**A**) Temperature dependence of the ellipticity of the native protein at 210 nm. (**B**) Temperature dependence of the ellipticity of the xylan binding domain at 230 nm. (**C**) Temperature dependence of the ellipticity of the native protein at 230 nm. (**D**) Temperature dependence of the ellipticity of the catalytic domain at 230 nm. The data shown were all acquired with samples dissolved in 50 mM phosphate buffer, pH 6.0. The solid lines represent the data actually acquired whereas the broken lines represent curves obtained by curve fitting (for details, see text).

unfolding of the catalytic and xylan binding domains of the intact enzyme are thermodynamically independent processes.

Thermodynamic Analysis

The following assumptions and procedures were employed in our analyses of the calorimetric data. First, it was assumed that the thermal unfolding of the catalytic and xylan binding domains of XlnA are independent processes. This assumption, which is compatible with our FTIR and CD data, enabled us to approximate the thermotropic behavior of the XlnA as a summation of two independent processes proceeding at equilibrium. Moreover, the irreversible thermal unfolding of XlnA was shown to be scan rate independent in the range between 18 and 44°C/h (data not shown). Based on the approach of Sanchez-Ruiz et al.,[28] our DSC thermograms were thus analyzed using the reversible two-state model to obtain the thermal unfolding thermodynamic parameters of XlnA. Second, it was also assumed that the thermal unfolding of the XBD does not result in protein aggregation under our conditions and thus that exothermic, aggregation-related thermal events do not contribute to any of the signals emanating from the unfolding of the XBD. This assumption is consistent with the FTIR spectroscopic data described above, our calorimetric studies of the reversibility of the isolated XBD, and the observation that idealized equilibrium DSC curves can be accurately fitted to the DSC thermograms exhibited by the XBD alone [see the broken line in Fig. 3(B)]. Finally, it was assumed that the thermal unfolding of the XlnA catalytic domain is not completely concurrent with the aggregation and precipitation of the protein, an assumption also consistent with the DSC and FTIR spectroscopic data described above. It was further assumed that because the unfolding process and the aggregation-related phenomena are not completely separated on the temperature scale the DSC endotherms arising from the thermal unfolding of the XCD will be distorted at higher

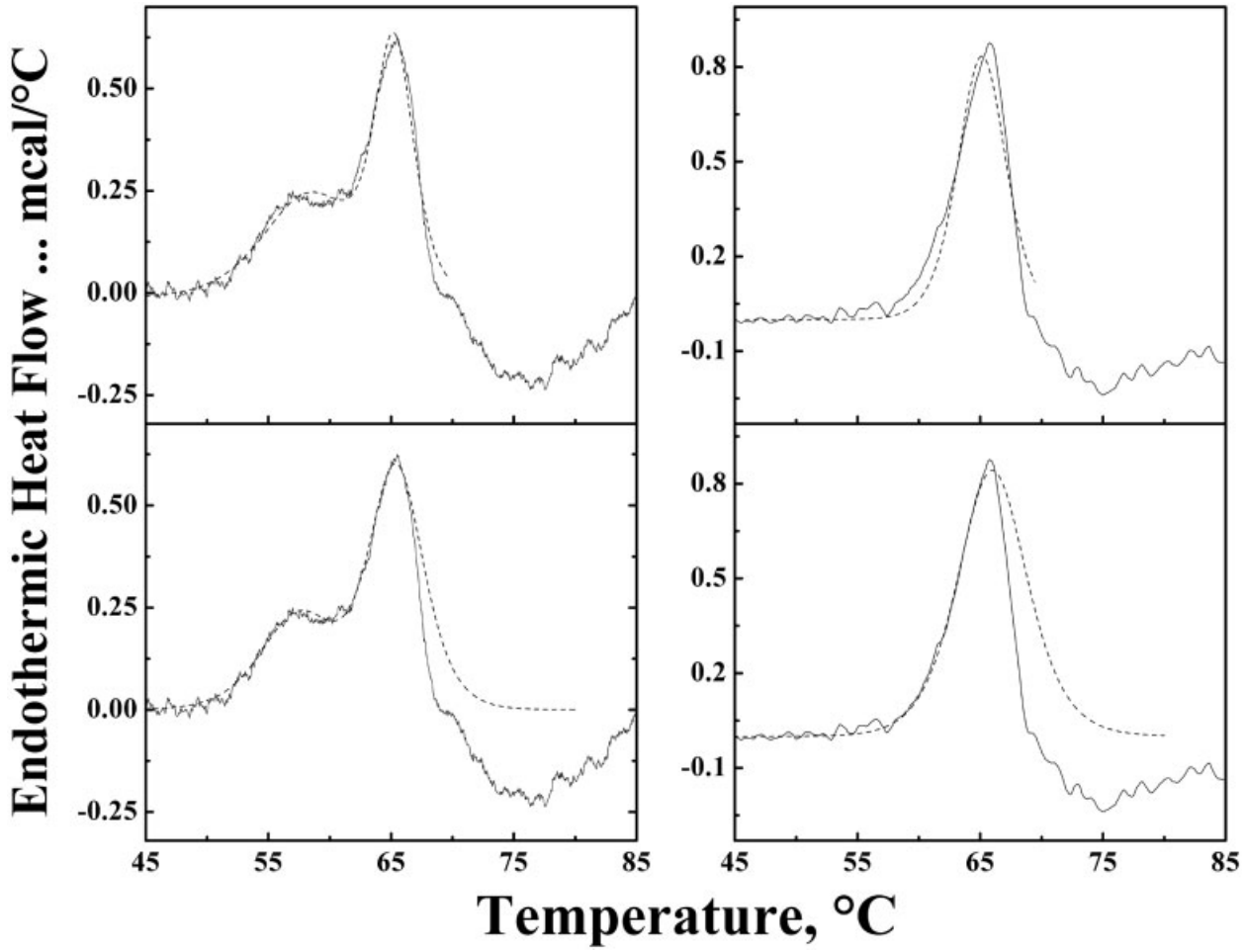

Fig. 8. DSC thermograms illustrating the curve-fitting procedures used to "correct" for the aggregation-related distortions of the unfolding endotherms of *S. lividans* XlnA (left) and its isolated catalytic domain (right). The baseline-corrected thermograms are indicated by the broken lines. The broken lines in the top panels show the results of fitting idealized DSC curves to the endotherms actually observed, whereas the broken lines in the bottom panels show the projected contours of the unfolding endotherms after correction for the effects of aggregation-related phenomena.

temperatures. The latter conclusion is supported by the observation that, in marked contrast to unfolding endotherms of the XBD, idealized equilibrium DSC curves cannot be accurately fitted to the DSC endotherms obtained from the XCD [see the broken line in Fig. 2(B)]. Given this, it was necessary to develop alternative procedures for obtaining estimates of the thermodynamic characteristics of the unfolding of the catalytic domain. The procedures employed here assume that distortions of the unfolding endotherms of the catalytic domain occur only at temperatures near the completion of the thermal unfolding process, an assumption supported by the FTIR spectroscopic data described above. Given this, data points from the terminal 30–40% of unfolding endotherms originating from the catalytic domain of XlnA were excluded and nonlinear least-squares minimization procedures were used to fit idealized DSC equilibrium curves to the rest of the data. Subsequently, the defining parameters of the fitted curves were used to describe the probable contours of the DSC endotherms free of aggregation-related distortion. The data illustrated in Figure 8 exemplify the results obtained using these general procedures.

The thermal unfolding of *S. lividans* xylanase A and its isolated domains was examined as a function of pH (range 4.0–9.0) in buffered media containing 50 mM NaCl. The thermal unfolding behavior of the native protein and its isolated subunits were found to be insensitive to the changes in buffer salt concentration from 5–500 mM NaCl. Our results indicate that, whether associated in the native protein or studied as isolated subunits, the thermal unfolding of the catalytic and xylan binding domains of the enzyme are differentially sensitive to changes in pH. As illustrated in Figure 9, the unfolding transition temperature (T_m) of the XCD is considerably more pH sensitive than that of the XBD, and it exhibits a fairly sharp maximum at pH values near 6.0. Also, the T_m of the XCD decreases asymmetrically upon deviation from its "optimal value," with the acidic side of its profile exhibiting a greater pH sensitivity (≈8°C per pH unit) than the alkaline side (≈5°C per pH unit). In contrast, the T_m of the XBD is less sensitive to pH, exhibits a broader pH maximum centered near pH 7.0, and its profile exhibits steeper changes in slope (≈5°C per pH unit) in the alkaline side of optimal. Because of the differential pH sensitivities of the

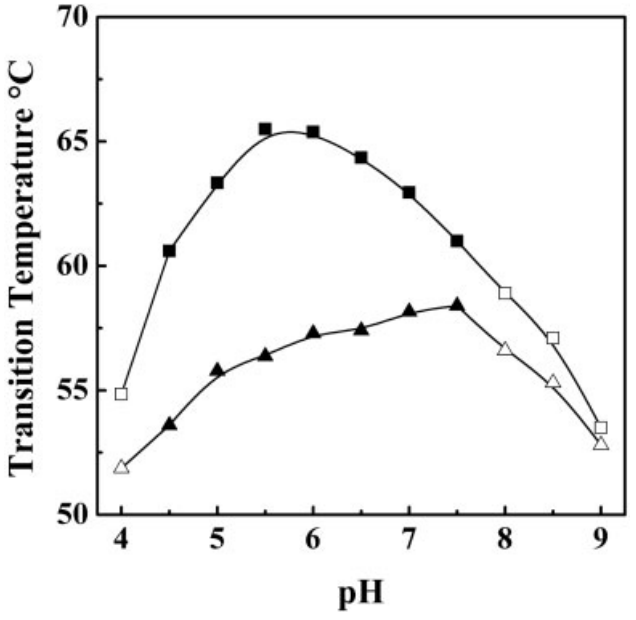

Fig. 9. pH dependence of the midpoint temperatures of the unfolding endotherms of *S. lividans* XlnA. Data are shown for the catalytic (squares) and xylan binding domains (triangles). Values represented by the open symbols were obtained from the inflection points of the DSC curves and those represented by the solid symbols were obtained from studies of the individual domains or from computer-assisted analysis (see text) of the unfolding endotherms exhibited by the native protein.

TABLE II. Characterization of the Thermal Unfolding Transitions of Xylanase A from *Streptomyces Lividans* (DSC Studies)[†]

	Data from the native protein			Data from the isolated domain		
pH	T_m (°C)	ΔH_{cal}	ΔH_{vh}	T_m (°C)	ΔH_{cal}	ΔH_{vh}
(A) Catalytic domain						
4.5	60.6	1100	557	60.6	1088	603
5.0	63.3	1435	594			
5.5	65.5	1444	623			
6.0	64.3	1398	690	64.4	1531	565
6.5	62.9	1393	632			
7.0	61.0	1331	728			
7.5				61.0	1423	594
(B) Xylan binding domain						
4.5	53.6	398	557	53.6	356	573
5.0	55.8	657	473			
5.5	56.4	552	531			
6.0	57.3	586	515	58.3	531	485
6.5	58.2	636	527			
7.0	58.4	741	552			
7.5				58.3	402	540

[†]ΔH_{cal}; calorimetric enthalpy (kJ/mol) estimated from the area under DSC endotherms; ΔH_{vh}; van't Hoff enthalpy (kJ/mol) estimated from the van't Hoff equation.

transition temperatures of the xylan binding and catalytic domains, separation between the observed thermal unfolding endotherms is maximal at pH values near 6.0 and diminishes markedly at both lower and higher pH values (see Fig. 9). Thus, at suboptimal pH the reduced resolution between the two thermal unfolding processes severely attenuated our capacity to extract accurate thermodynamic parameters from the data obtained with the native protein. Under our conditions, we found that the pH range over which such thermal unfolding data could be reliably deconvolved by the procedures outlined above is limited to pH values between 4.5 and 7.0.

Despite the aforementioned limitations, several interesting observations emerge from an examination of the thermodynamic parameters calculated from our DSC studies. First, it is clear that the thermodynamic parameters obtained from the native protein are essentially similar to those of the isolated domains (see Table II). This observation provides some validation for the analytic procedures used to extract the thermodynamic parameters from the experimental data and lends further support to the idea that the thermal unfolding of the XCD and XBD are independent processes that are unaffected by their association in the native protein. Second, the calorimetric enthalpy values calculated from the area under the unfolding endotherms of the XBD are, within the estimated experimental error (≈10%), comparable in magnitude to the corresponding van't Hoff enthalpy values (i.e., those derived by calculation from the widths of the endothermic transitions). This pattern of behavior is usually observed with small compact globular proteins whose thermal unfolding approaches that of a unimolecular two-state process proceeding at equilibrium.[29] Thus, the thermal unfolding of the XBD of this enzyme can be approximated by a unimolecular two-state process in which all structural regions of the protein unfold as a single domain. Third, the calorimetric enthalpy associated with the thermal unfolding of the XCD is approximately twice as large as the corresponding van't Hoff enthalpy of this process (see Table II), indicating that the thermal unfolding of the catalytic domain is not a simple cooperative two-state process. Similar observations have been noted in DSC studies of the thermal unfolding of the Bence–Jones protein, in which case evidence was presented that such behavior derived from the presence of two subdomains that unfolded independently of each other.[30] The possibility that the single unfolding endotherm resolved in our DSC studies of the catalytic domain may also be the result of the independent unfolding of at least two subdomains over a similar temperature range is explored further in the discussion.

An analysis of the temperature-dependent changes in the far-UV ellipticities of the *S. lividans* XlnA was also performed to obtain additional information on the thermodynamic properties of the unfolding process. Implicit to our analyses are the assumptions that the observed change in molar ellipticity is directly proportional to the degree of unfolding and that thermal unfolding can be approximated by a two-state process proceeding at equilibrium. Also, given the calorimetric observations, we assumed that aggregation-related phenomena may distort the observations at temperatures well above the range of the unfolding transition and our analyses were therefore restricted to CD data obtained close to the initiation and completion temperatures of the unfolding transition. Also, these studies were performed on data acquired at 210 nm. This

TABLE III. Characterization of the Thermal Unfolding Transitions of Xylanase A from *Streptomyces Lividans* (CD Studies)[†]

pH	T_m (°C)	ΔH (kJ/mol)
3.98	59.1	598
4.49	63.8	544
5.00	67.6	640
5.50	68.7	569
6.00	69.2	582
6.49	68.2	565
7.00	66.7	611
7.46	64.9	603
8.01	62.3	703
8.57	57.4	682
9.02	54.1	657

[†]CD studies were carried out at 210 nm (thermal unfolding of the catalytic domain).

wavelength was chosen because the thermal unfolding of the XBD is transparent at this wavelength. While thermal unfolding of the two domains of XlnA can be observed at 230 nm, these two processes mask each other, making an accurate evaluation of the thermodynamic parameters impossible.

The data listed in Table III were derived from an analysis of the temperature dependence of the molar ellipticity of the native protein. For the reasons given above, these results pertain only to the thermal unfolding of the catalytic domain. Also, because the data were derived essentially from an analysis of the shape of the thermal unfolding profile, the enthalpy values obtained are the equivalent of the van't Hoff enthalpy values determined in the DSC experiment. Overall, the data show a pattern that is essentially similar to that observed by DSC. Moreover, the pattern of pH sensitivity and the magnitude of the van't Hoff enthalpy values calculated from the CD experiment are essentially the same as those determined by DSC. The thermodynamic picture emerging from these CD studies is therefore comparable to that deduced from the DSC data presented above.

DISCUSSION

A major finding of this work is that native *S. lividans* XlnA is an assembly of two distinct domains with markedly different structural and functional properties. Similar results were reported in earlier studies of *Streptomyces halstedii* JM8 xylanases Xys1L and Xys1S[31] and of *Cellulomonas fimi* Cex,[32] enzymes that also belong to the glycosyl hydrolase family 10 and whose domain organizations appear to be similar to that of *S. lividans* XlnA . Our results are also compatible with those obtained in studies of the thermal unfolding of xylanases obtained from the hyperthermophilic bacterium *Thermotoga maritime.*[21] This work also demonstrates that with *S. lividans* XlnA, differences between the N-terminal catalytic and C-terminal substrate binding domains are manifest in their secondary structure and thermal stability as well as in their pH sensitivity. Our results also suggest that there are significant differences between the mechanisms by which the catalytic and xylan binding domains of this enzyme unfold. With the XBD, van't Hoff enthalpy values estimated by DSC are comparable in magnitude, although not identical, to the calorimetric enthalpy values determined, suggesting that the unfolding of *S. lividans* XBD occurs as a single-domain process. However, with the XCD the calorimetric enthalpy of the single unfolding endotherm resolved by DSC is approximately twice the van't Hoff enthalpy values estimated by both CD and DSC, suggesting that the unfolding endotherm probably arises from the independent unfolding of two subdomains over a similar temperature range. Similar results were obtained in the case of pepsinogen, a protein composed of two structural subunits that unfold independently of each other,[33] but—to our knowledge—the existence of subdomains such as proposed here has not been reported in any of the other family 10 glycosyl hydrolases. The possible existence of such subdomains may also seem surprising when viewed within the context of the single-crystal X-ray diffraction structure, which indicates virtually all of the amino acids of *S. lividans* XlnA2 are folded into a so-called $(\alpha/\beta)_8$ motif.[12] However, Derewenda et al.[12] also noted that the *S. lividans* XlnA2 α/β barrel is atypical in structure and that it is the most elliptically shaped of all the α/β-barrel motifs studied so far. The highly elliptical nature of the α/β-barrel motif adopted by this protein could be the structural basis of the two putative unfolding subdomains alluded to above because it creates a two-fold axis of symmetry in the arrangement of the elements of the $(\alpha/\beta)_8$ barrel about which subdomains can, in principle, exist. The resolution of this issue will clearly require more detailed structural studies that are outside the scope of the physical techniques applied here.

Finally, we note that, once unfolded, the fates of the catalytic and xylan binding domains of *S. lividans* XlnA are different. In these studies we find that although thermal unfolding of the XBD of this enzyme can lead to the inactivation of its function, the process is slow at temperatures below 69°C and does not normally result in aggregation and precipitation of the protein. Moreover, under our conditions, near maximal refolding of the XBD to its native state occurs when the unfolded samples of the XBD are cooled from temperatures below 69°C. The latter observation further suggests that *S. lividans* XBD is probably fairly durable, a property likely to be valuable industrially. With the XCD, however, the unfolding process initiates events that eventually result in the aggregation and precipitation of the protein. With this domain, the latter processes are manifested by the exothermic events that commence at temperatures near to the completion of the calorimetrically resolved unfolding endotherm. Such processes have been observed with at least one other xylanase.[32] Although the initial thermal unfolding of such proteins are probably reversible processes, the unfolding event itself is soon followed by other processes that eventually cause an irreversible inactivation of its function and, in many cases, aggregation and precipitation of the protein. The latter events can be attributed to the exposure of hydrophobic surfaces that are normally shielded from the aqueous environment. The fact that this and other xylanases seem predisposed to such behavior is of special

concern to the potential industrial applications of these enzymes. The engineering of xylanase mutants that are more resistant to such behavior is one of the goals of this research project.

ACKNOWLEDGMENTS

The authors are indebted to Dr. Cyril M. Kay of the Department of Biochemistry of the University of Alberta for his many helpful discussions and his assistance in analysis and interpretation of the CD data.

REFERENCES

1. Jeffries TW. Enzymatic treatment of pulp. In: Rowell RM, Schultz TP, Noryan R, Editors. Emerging Technologies for Materials and Chemicals from Biomembranes. ACS Symposium Series 476; Washington, DC: ACS; 1992. p 313–329.
2. Henrissat B. Cellulases and their interaction with cellulose. Cellulose 1994;1:169–196.
3. Viikari L, Kantelinen A, Sundquist J, Linko M. Xylanases in bleaching—from an idea to the industry. FEMS Microbiol Rev 1994;13:335–350.
4. Morosoli R, Bertrand J-L, Mondou, F, Shareck, F, Kluepfel D. Purification and properties of a xylanase from *Streptomyces lividans*. Biochem J 1986;239:587–592.
5. Roberge M, Shareck F, Morosoli R, Kluepfel D, Dupont C. Characterization of two important histidine residues in the active site of xylanase A from *Streptomyces lividans*, a family 10 glycanase. Biochemistry 1997;36:7769–7775.
6. Bertrand J-L, Morosoli R, Shareck F, Kluepfel D. Expression of the xylanase gene of *Streptomyces lividans* and production of the enzyme on natural substrates. Biotech Bioeng 1989;33:791–794.
7. Shareck F, Roy C, Yaguchi M., Morosoli R, Kluepfel D. Sequences of three genes specifying xylanases in *Streptomyces lividans.* Gene 1991;107:75–82.
8. Moreau A, Roberge M, Manin C, Shareck F, Kluepfel D, Morosoli R. Identification of two acidic residues involved in the catalysis of xylanase A from *Streptomyces lividans.* Biochem J 1994;302:291–295.
9. Moreau A, Shareck F, Kluepfel D, Morosoli R. Alteration of the cleavage mode and of the transglycosylation reaction of the xylanase A of *Streptomyces lividans* 1326 by site-directed mutagenesis of the Asn173 residue. Eur J Biochem 1994;219:261–266.
10. Roberge M, Shareck F, Morosoli R, Kluepfel D, Dupont C. Site-directed mutagenesis study of histidine 86 of xylanase A from *Streptomyces lividans*, a conserved residue in family 10 glycanases. Protein Eng 1998;11:399–404.
11. Dupont C, Roberge M, Shareck F, Morosoli R, Kluepfel D. Substrate-binding domains of glycanases from *Streptomyces lividans*. Characterization of a new family of xylan-binding domains. Biochem J 1998;330:41–45.
12. Derewenda U, Swenson L, Green R, Wei Y, Morosoli R, Shareck F, Kluepfel D, Derewenda ZS. Crystal structure at 2.6 Å resolution of the *Streptomyces lividans* xylanase A, a member of the F family of β-1, 4-glycanases. J Biol Chem 1994;269:20811–20814.
13. White A, Withers SG, Gilkes NR, Rose RD. Crystal structure of the catalytic domain of the β-1,4-glycanase Cex from *Cellulomonas fimi.* Biochemistry 1994;33:12546–12552.
14. Xu G-Y, Ong E, Gilkes NR, Kilburn DG, Muhandiram, DR, Brandts MH, Carver JP, Kay LE, Harvey TS. .Solution structure of a cellulose-binding domain from *Cellulomonas fimi* by nuclear magnetic resonance spectroscopy. Biochemistry 1995;34:6993–7008.
15. Freire E. Thermal denaturation methods in the study of protein folding. Meth Enzymol 1995;259:144–168.
16. Gill SS, von Hippell PH. Calculation of protein extinction coefficients from amino acid sequence data. Anal Biochem 1989;182: 319–326.
17. Mantsch HH, Madec C, Lewis, RNAH, McElhaney RN. Thermotropic phase behavior of model membranes composed of phosphatidylcholines containing iso-branched fatty acids. 2. Infrared and ^{31}P-NMR spectroscopic studies. Biochemistry 1985;24:2440–2446.
18. Pace CN, Shirley BA, Thomson JA. Measuring the conformational stability of a protein. In: Creighton TE, Editor. Protein Structure: A Practical Approach. Oxford, UK: Oxford University, IRL Press; 1989. p 311–330.
19. Middaugh CR, Mach H, Ryan JA, Sanyal G, Volin DB. Infrared spectroscopy. In: Shirley BA, Editor. Methods in Molecular Biology, Protein Stability and Folding: Theory and Practice; Totowa, NJ: Humana Press; 1995. p 137–156.
20. Pribic R, van Stokkum IHM, Chapman D, Haris PI, Bloemendal M. Protein secondary structure from Fourier transform infrared and/or circular dichroism spectra. Anal Biochem 1993;214:366–378.
21. Wassenberg D, Schurig H, Liebl W, Jaenicke R. Xylanase XynA from the hyperthermophilic bacterium *Thermotoga maritima*: structure and stability of the recombinant enzyme and its isolated cellulose-binding domain. Protein Sci 1997;6:1718–1726.
22. Khan MY, Villanueva G, Neuman SA. On the origin of the positive band in the far-ultraviolet circular dichroic spectrum of fibronectin. J Biol Chem 1989;264:2139–2142.
23. Woody RW. Contributions of tryptophan side chains to the far ultraviolet circular dichroism of proteins. Eur Biophys J 1994;23: 253–262.
24. Kraulis PJ, Clore GM, Nikges M, Jones TA, Pettersson G, Knowles J, Gronenborn AM. Determination of the three-dimensional structure of the C-terminal domain of cellobiohydrolase I from *Trichoderma reesei*. A study using nuclear magnetic resonance and hybrid distance geometry-dynamical simulated annealing. Biochemistry 1989;28:7241–7257.
25. Xu GY, Ong E, Gilkes NR, Kilburn DG, Muhandiram, DR, Harris-Brandts M, Carver J, Kay LE, Harvey TS. Solution structure of a cellulose-binding domains from *Cellulomonas fimi* by nuclear magnetic resonance spectroscopy. Biochemistry 1995; 34:6993–7009.
26. Johnson PE, Joshi MD, Tomme P, Kilburn DG, McIntosh LP. Structure of the N-terminal cellulose-binding domain of *Cellulomonas fimi* CenC determined by nuclear magnetic resonance spectroscopy. Biochemistry 1996;35:14381–14394.
27. Tormo J, Lamed R, Chirino AJ, Morag E, Bayer EA, Sholam Y, Steitz TA. Crystal structure of a bacterial family-III cellulose binding domain: a general mechanism for attachment to cellulose. EMBO J 1996;15:5739–5751.
28. Sanchez-Ruiz JM, Lopez-Lacomba JL, Cortijo M, Mateo PL. Differential scanning calorimetry of the irreversible thermal denaturation of thermolysin. Biochemistry 1988;27:1648–1652.
29. Privalov PL, Khechinashvili NN. A thermodynamic approach to the problem of stabilization of globular protein structure: a calorimetric study. J Mol Biol 1974;83:665–684.
30. Zavyalov VP, Trotsky GV, Khechinashvili NN, Privalov PL. Thermally induced conformational transitions of Bence–Jones protein IVA and its proteolytic fragments. Biochim Biophys Acta 1977;492:102–111.
31. Ruiz-Arribas A, Santamaria RI, Zhadan GG, Villar E, Shnyrov VL. Differential scanning calorimetric study of the thermal stability of xylanase from *Streptomyces halstedii* JM8. Biochemistry 1994;33:13787–13791.
32. Nikolova PV, Creagh AL, Duff SJB, Haynes CA. Thermostability and irreversible activity loss of exoglucanase/xylanase Cex from *Cellulomonas fini*.. Biochemistry 1997;36;1381–1388.
33. Privalov PL, Mateo PL, Khechinashvili NN. Comparative thermodynamic study of pepsinogen and pepsin structure. J Mol Biol 1981;153:445–464.